c-axis optical sum in underdoped superconducting cuprates

J. P. Carbotte[1,2] and E. Schachinger[3,*]

[1]*Department of Physics and Astronomy, McMaster University, Hamilton, Ontario, Canada N1G 2W1*

[2]*The Canadian Institute for Advanced Research, Toronto, Ontario, Canada M5G 1Z8*

[3]*Institute of Theoretical and Computational Physics, Graz University of Technology, A-8010 Graz, Austria*

(Received 6 November 2012; revised manuscript received 10 December 2012; published 21 December 2012)

In conventional metals, the total optical spectral weight under the real part of the dynamical conductivity remains unchanged in going from normal to superconducting state. In the underdoped cuprates, however, experiments found that the interlayer conductivity no longer respects this sum rule. Here, we find that a recently proposed phenomenological model of the pseudogap state which is based on ideas of a resonating valence bond spin liquid naturally leads to such a sum-rule violation. For the interplane charge transfer, a coherent tunneling model is used. We also obtain analytic results based on a simplification of the theory which reduces it to an arc model. This provides further insight into the effect of the opening of a pseudogap on the *c*-axis optical conductivity $\mathrm{Re}[\sigma_c(\omega)]$. The missing area under $\mathrm{Re}[\sigma_c(\omega)]$ normalized to the superfluid density, which is found to be one in the Fermi-liquid limit with no pseudogap, is considerably reduced when the pseudogap becomes large and the size of the Luttinger pockets or arcs is small.

DOI: 10.1103/PhysRevB.86.224512 PACS number(s): 74.20.Mn, 74.72.Kf

I. INTRODUCTION

Sum rules are useful in analyzing and understanding data on the dynamic conductivity $\sigma(\omega)$. The area under the real part of $\sigma(\omega)$ is related to the square of the plasma frequency which plays a central role in optical absorption.[1] For superconductors, the Ferrell-Glover-Tinkham (FGT) sum rule[2,3] states that the missing area under $\mathrm{Re}[\sigma(\omega \geqslant 0^+)]$ which comes from the quasiparticle excitations is to be found in a δ distribution at zero frequency with its weight related to the superfluid stiffness of the condensate. The *c*-axis optical response of the underdoped cuprates is, however, different and substantial violations of the FGT sum rule have been observed.[4] Such violations have been interpreted as an indication of non-Fermi-liquid behavior of the in-plane charge dynamics[5–12] possibly due to the preformed pair mechanism[7] in which the gap remains above the superconducting critical temperature T_c, but without coherence between the Cooper pairs, or the hole mechanism of superconductivity,[8,9] or the interlayer tunneling model.[10–12] Effects of an in-plane magnetic field **H** on the FGT sum rule have also been studied[13] as well as the vortex state when **H** is oriented along the *c*-axis perpendicular to the CuO_2 planes.[14]

It is well known that in the underdoped cuprates, a pseudogap feature[15] associated with the emergence of a new energy scale[16] appears in their normal state above the superconducting dome. Many ideas have been put forward as the origin of this phenomenon such as preformed pairs[17,18] or a (*d*-density wave) competing order.[19,20] More recently the phenomenological self-energy introduced by Yang *et al.*[21] (YRZ) has gained prominence as it has become realized that it provides a simple and robust explanation[22–31] of the previously believed anomalous properties of the cuprate phase diagram. The YRZ model is based on the ideas of the resonating valence bond spin liquid by Anderson.[32] It features a quantum critical point (QCP) below which a pseudogap emerges, and this leads to a reconstruction of the large Fermi surface (FS) of Fermi-liquid theory into Luttinger hole pockets about the nodal direction in the CuO_2 Brillouin zone (BZ) as the antiferromagnetic Mott insulating state is approached. The remarkable success of the YRZ ansatz to provide a first understanding of the superconducting properties of the underdoped state indicates that, however simplified it may be, it captures an essential element which needs to be added to conventional BCS theory. The emergence of a pseudogap goes beyond and is quite different from other extensions of BCS theory which have been found important in dealing with real conventional superconductors. These include so-called strong-coupling effects[33–35] which have their root in Eliashberg theory, anisotropies[36–38] entering the electron-phonon interaction as well as, in some materials, energy dependence in their electronic density of states.[39–42]

In this paper, we study how the growth of a pseudogap in the YRZ model affects the *c*-axis optical sum rule. In Sec. II, we present a Green's function formulation of the optical sum rule for the transverse direction. A brief description of the YRZ model is given in Sec. III. Numerical results are found in Sec. IV. In Sec. V, we consider the limit of the YRZ model which corresponds to an arc model for which we can get a simplified analytic formula for the *c*-axis sum rule. This helps greatly in our understanding of the physics behind the sum-rule violation found in this work. A summary and conclusions are found in Sec. VI.

II. FORMALISM FOR OPTICAL SUM

In terms of the interplane tunneling matrix element for the transfer along the *c*-axis of an electron of momentum **k** in one plane to **p** in the adjacent plane $t_{\mathbf{k},\mathbf{p}}$,[43–47] the out-of-plane sum rule[5–7] reads as

$$\frac{N_n - N_s}{\rho_s} = \frac{1}{2} + \frac{1}{2}\frac{\sum_{\omega_n}\sum_{\mathbf{k},\mathbf{p}}|t_{\mathbf{k},\mathbf{p}}|^2[G_s(\mathbf{k},i\omega_n)G_s(\mathbf{p},i\omega_n) - G_n(\mathbf{k},i\omega_n)G_n(\mathbf{p},i\omega_n)]}{\sum_{\omega_n}\sum_{\mathbf{k},\mathbf{p}}|t_{\mathbf{k},\mathbf{p}}|^2 F(\mathbf{k},i\omega_n)F(\mathbf{p},i\omega_n)}. \quad (1)$$

In this equation, $\sum_{\omega_n}$ is a sum over fermion Matsubara frequencies at temperature T, $G_s(\mathbf{k},i\omega_n)$ is the in-plane charge carrier Green's function in the superconducting state with $G_n(\mathbf{k},i\omega_n)$ its normal-state limit, and $F(\mathbf{k},i\omega_n)$ is the anomalous Gor'kov Green's function describing the Cooper-pair condensate. The c-axis optical spectral weight in the superconducting and normal state, respectively, is defined as the area under the real part of the dynamic transverse (between the planes) conductivity $\sigma_c(T,\omega)$, namely,

$$N_n = \int_{0^+}^{\infty} d\omega\, \mathrm{Re}[\sigma_{c,n}(T,\omega)] \tag{2a}$$

and

$$N_s = \int_{0^+}^{\infty} d\omega\, \mathrm{Re}[\sigma_{c,s}(T,\omega)]. \tag{2b}$$

Finally, ρ_s is the c-axis superfluid density in units such that the FGT sum rule would correspond to $N_n - N_s = \rho_s$ with ρ_s related to the denominator of the second term in Eq. (1). Here, we will take a coherent tunneling model for the matrix element $t_{\mathbf{k},\mathbf{p}}$.[5–7] Consideration of the geometrical arrangement of the CuO_2 atoms in a particular plane and its directly adjacent neighbor leads to a model for $t_{\mathbf{k},\mathbf{p}}$ which takes on the form[48–52] (see Fig. 1)

$$t_{\mathbf{k},\mathbf{p}} = t_\perp \delta_{\mathbf{k},\mathbf{p}} [\cos(k_x a) - \cos(k_y a)]^2, \tag{3}$$

where $t_\perp$ is a constant, the Kronecker delta conserves momentum parallel to the plane, and a is the in-plane lattice constant. The form (3) means that the probability of c-axis tunneling of the quasiparticles of the CuO_2 plane around the nodal direction is greatly reduced and this leads to a much less metallic response in c than in the a-b direction. The conductivity sum of Eq. (1) now reads as

$$\frac{N_n - N_s}{\rho_s} = \frac{1}{2} + \frac{1}{2} H, \tag{4}$$

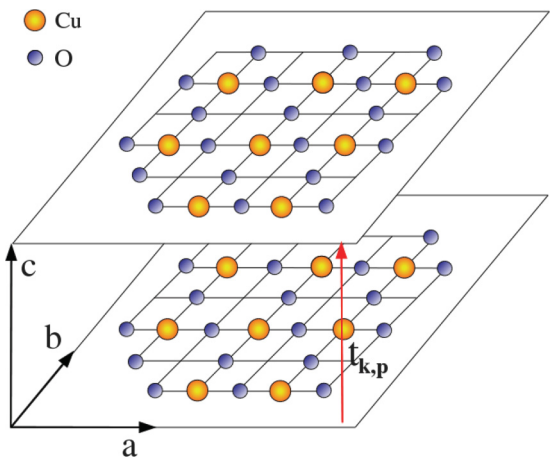

FIG. 1. (Color online) The transport between CuO_2 planes is assumed to proceed through a coherent matrix element $t_{\mathbf{k},\mathbf{p}} = t_\perp \delta_{\mathbf{k},\mathbf{p}} [\cos(k_x a) - \cos(k_y a)]^2$.

with

$$H = \frac{\sum_{\omega_n} \sum_{\mathbf{k}} \eta^4(\mathbf{k}) \left[G_s^2(\mathbf{k},i\omega_n) - G_n^2(\mathbf{k},i\omega_n) \right]}{\sum_{\omega_n} \sum_{\mathbf{k}} \eta^4(\mathbf{k}) |F(\mathbf{k},i\omega_n)|^2}. \tag{5}$$

Here,

$$\eta(\mathbf{k}) = [\cos(k_x a) - \cos(k_y a)]/2. \tag{6}$$

Central to this work is Eq. (5) in the pseudogap model of Yang *et al.*,[21] to which we now turn.

III. PHENOMENOLOGICAL YRZ MODEL

Yang *et al.*[21] give an ansatz for the coherent part of the Green's function in the pseudogap state which applies to the underdoped cuprates for doping x below a critical value x_c which represents the quantum critical point (QCP) below which the pseudogap forms and the large Fermi surface of Fermi-liquid theory is reconstructed into Luttinger pockets. Their ansatz which finds some justification in the theory of correlated doped spin liquids of an array of two-legged Hubbard ladders[21] is

$$G_s(\mathbf{k},\omega,x) = \sum_{\alpha=\pm} \frac{g_t(x) W_{\mathbf{k}}^{\alpha}}{\omega - E_{\mathbf{k}}^{\alpha} - \Delta_{sc}^2(\mathbf{k},x) \big/ \left(\omega + E_{\mathbf{k}}^{\alpha}\right)}, \tag{7}$$

where $E_{\mathbf{k}}^{\pm} = (\xi_{\mathbf{k}} - \xi_{\mathbf{k}}^0)/2 \pm E_{\mathbf{k}}$, $E_{\mathbf{k}} = \sqrt{\tilde{\xi}_{\mathbf{k}}^2 + \Delta_{pg}^2(\mathbf{k},x)}$, $\tilde{\xi}_{\mathbf{k}} = (\xi_{\mathbf{k}} + \xi_{\mathbf{k}}^0)/2$, and the weights $W_{\mathbf{k}}^{\pm} = (1 + \tilde{\xi}_{\mathbf{k}}/E_{\mathbf{k}})/2$. The band energies on which the model is based are those for $Ca_2CuO_2Cl_2$ and we will not change these here. They can be written as $\xi_{\mathbf{k}} = -2t(x)[\cos(k_x a) + \cos(k_y a)] - 4t'(x)\cos(k_x a)\cos(k_y a) - 2t''(x)[\cos(2k_x a) + \cos(2k_x a)] - \mu$, where μ is the chemical potential and the renormalized band parameters are $t(x) = g_t(x)t_0 + 3g_s(x)J\chi/8$, $t'(x) = g_t(x)t_0'$, $t''(x) = g_t(x)t_0''$, with t_0 the unrenormalized first-neighbor hopping parameter, $J/t_0 = \frac{1}{3}$, $\chi = 0.338$, $t_0'/t_0 = -0.3$, and $t_0''/t_0 = 0.2$. The energy $\xi_{\mathbf{k}}^0$ is obtained from $\xi_{\mathbf{k}}$ setting all higher-order hopping $t_0' = t_0'' = 0$. Results can be presented in units of t_0 which is sometimes taken to be 170 meV for illustrative purposes. The Gutzwiller factors are

$$g_t(x) = \frac{2x}{1+x} \quad \text{and} \quad g_s(x) = \frac{4}{(1+x)^2}. \tag{8}$$

The x dependence of this renormalized band is such that they narrow on approach to the Mott insulating state. Note that the Gutzwiller factor $g_t(x)$ also appears directly in $G(\mathbf{k},\omega,x)$ [Eq. (7)], and this reduces the weight of the coherent part of the electron spectral density as correlations increase and the system becomes more incoherent. Both superconducting and pseudogap have d-wave symmetry with

$$\Delta_{sc}(\mathbf{k},x) = \Delta_{sc}^0(x)[\cos(k_x a) - \cos(k_y a)]/2 \tag{9a}$$

and

$$\Delta_{pg}(\mathbf{k},x) = \Delta_{pg}^0(x)[\cos(k_x a) - \cos(k_y a)]/2. \tag{9b}$$

The gap amplitudes as a function of doping are $\Delta_{sc}^0/t_0 = 0.14[1 - 82.6(x - 0.2)^2]$ and $\Delta_{pg}^0/t_0 = 0.6[1 - x/0.2]$. Here, we take the superconducting dome for $\Delta_{sc}^0(x)$ to reflect the experimental observations for the variation of the superconducting critical temperature T_c as a function of x with two modifications. This is shown in Fig. 2(a). Optimum doping

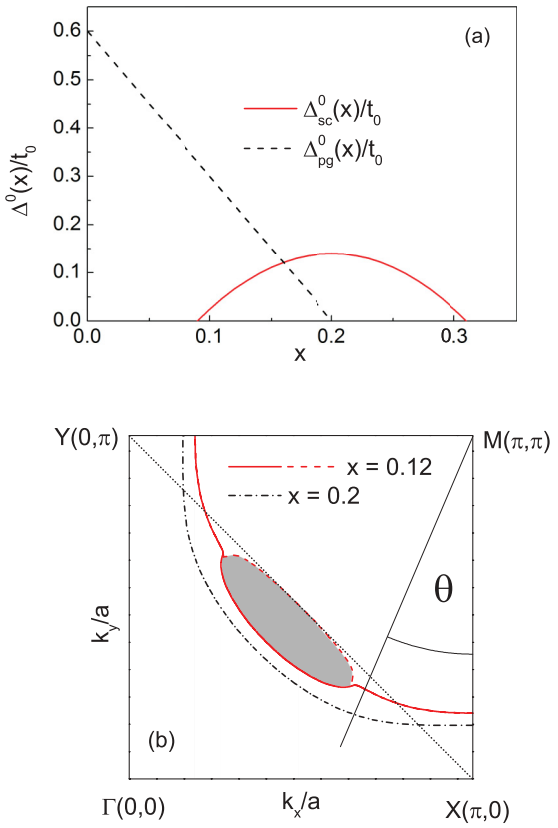

FIG. 2. (Color online) (a) The superconducting gap amplitude Δ^0_{sc} [solid (red) line] and the pseudogap amplitude Δ^0_{pg} [dashed (black) line] in units of t_0 as a function of doping x. (b) Large Fermi surface of Fermi-liquid theory for $x = 0.2$ [dashed-dotted (black) line] and reconstructed Fermi surface for $x = 0.12$ [solid and dashed (red) lines].

is taken at $x = 0.2$ rather than the experimental value of 0.16. This is the model used by YRZ and we will not modify it here. The second modification is that, guided by experimental findings, we will take for definiteness the gap to T_c dimensionless ratio $2\Delta(0)/(k_B T_c) = 6$ rather than the canonical BCS value of 4.3 for d-wave symmetry. From Eq. (7), we can determine in the usual way the regular $A(\mathbf{k},\omega)$ and anomalous $B(\mathbf{k},\omega)$ spectral functions

$$A(\mathbf{k},\omega) = \sum_{\alpha=\pm} g_t(x) W^\alpha_{\mathbf{k}} \{(u^\alpha)^2 \delta[\omega - E^\alpha_s(\mathbf{k})] + (v^\alpha)^2 \delta[\omega + E^\alpha_s(\mathbf{k})]\} \tag{10}$$

and

$$B(\mathbf{k},\omega) = \sum_{\alpha=\pm} g_t(x) W^\alpha_{\mathbf{k}} \frac{\Delta_{sc}(\mathbf{k},x)}{2E^\alpha_s(\mathbf{k})} \{\delta[\omega - E^\alpha_s(\mathbf{k})] - \delta[\omega + E^\alpha_s(\mathbf{k})]\}, \tag{11}$$

with

$$(u^\alpha)^2 = \frac{1}{2}\left[1 + \frac{E^\alpha_{\mathbf{k}}}{E^\alpha_s(\mathbf{k})}\right] \tag{12a}$$

and

$$(v^\alpha)^2 = \frac{1}{2}\left[1 - \frac{E^\alpha_{\mathbf{k}}}{E^\alpha_s(\mathbf{k})}\right], \tag{12b}$$

where

$$E^\alpha_s(\mathbf{k}) = \sqrt{\left(E^\alpha_{\mathbf{k}}\right)^2 + \Delta^2_{sc}(\mathbf{k},x)}. \tag{13}$$

This specifies completely our model based on the work of Yang *et al.*[21] In Fig. 2(b), we present our normal-state results $\Delta_{sc}(\mathbf{k},x) = 0$ for the reconstructed Fermi surface brought about by the opening of the pseudogap in the case $x = 0.12$ [solid and dashed (red) lines] and compare to the case of optimum doping $x = 0.2$ [dashed-dotted (black) curve] which also coincides with the QCP at which the pseudogap first opens in Ref. 21. Of course, in experiments the QCP for the growth of the pseudogap [dashed (black) line] is not necessarily the same point as optimum doping, that is, the maximum in the superconducting gap [solid (red) curve]. In the phase diagram of Hüfner *et al.*,[16] which is based on considerations of many different data sets involving different techniques such as scanning tunneling microscopy (STM), angular-resolved photoemission spectroscopy (ARPES), optical conductivity, and Raman, the QCP is found to reside at the overdoped end of the phase diagram of Fig. 2(a). For simplicity, we retain here the phase diagram of YRZ as shown in Fig. 2(a). Returning to Fig. 2(b), the dashed-dotted (black) line represents the large Fermi surface of Fermi-liquid theory for $x = 0.2$, while the shaded (gray) region depicts the Luttinger hole pocket with Fermi contours on both sides of the pocket but that facing the antiferromagnetic BZ boundary [dotted (black) line] carries a weak weighting factor as compared with the other side, which gives a Fermi arc. Beyond this arc, there are no zero-energy excitations and the rest of the contour is gaped and represents a contour of nearest approach for a given direction defined by the angle θ with its origin at $M(\pi,\pi)$. As x is decreased further, the Luttinger contour shrinks and there are fewer and fewer states with zero excitation energy and this implies a reduction in metallicity as we approach half filling, i.e., $x = 0$.

IV. NUMERICAL EVALUATION

Central to our work is the calculation of the quantity H [Eq. (5)]. We can write the Green's functions $G(\mathbf{k},i\omega_n)$ and $F(\mathbf{k},i\omega_n)$ in terms of their spectral representations $A(\mathbf{k},\nu)$ and $B(\mathbf{k},\nu)$ as

$$G(\mathbf{k},i\omega_n) = \int_{-\infty}^{\infty} d\nu \, \frac{A(\mathbf{k},\nu)}{i\omega_n - \nu} \tag{14}$$

with a similar form for the anomalous Gor'kov function. We obtain

$$T\sum_{\omega_n} G(\mathbf{k},i\omega_n) G(\mathbf{k}',i\omega_n) = \int_{-\infty}^{\infty} \frac{d\nu \, d\nu'}{\nu - \nu'} [f(\nu) - f(\nu')] A(\mathbf{k},\nu) A(\mathbf{k}',\nu') \tag{15}$$

and want the case $\mathbf{k}' \to \mathbf{k}$. Here, $f(\nu)$ is the Fermi-Dirac distribution function at temperature T. For zero temperature, $f(\nu) = 1$ for $\nu < 0$ and zero for $\nu > 0$ and can be written in terms of the Heaviside θ function. To illustrate the algebraic

steps involved in writing H in terms of the spectral densities rather than Green's functions themselves, we consider first the normal pseudogap state, i.e. the case $\Delta_{sc} = 0$. Its contribution to H involves

$$T\int \frac{d^2k}{(2\pi)^2}\,\eta^4(\mathbf{k})\sum_{\omega_n}\left[G_n^0(\mathbf{k},i\omega_n)\right]^2 = \int \frac{d^2k}{(2\pi)^2}\eta^4(\mathbf{k})\left\{g_t(x)^2\left[\sum_{\alpha=\pm}\left(W_{\mathbf{k}}^{\alpha}\right)^2\frac{\partial f\left(E_{\mathbf{k}}^{\alpha}\right)}{\partial E_{\mathbf{k}}^{\alpha}} + 2W_{\mathbf{k}}^{+}W_{\mathbf{k}}^{-}\frac{f(E_{\mathbf{k}}^{+}) - f(E_{\mathbf{k}}^{-})}{E_{\mathbf{k}}^{+} - E_{\mathbf{k}}^{-}}\right]\right\}. \quad (16)$$

The first term on the right-hand side of Eq. (16) involves intraband transitions and the second is interband. We have taken the limit $\mathbf{k}' \to \mathbf{k}$ and recognized that the denominator in the interband case can vanish at most on a set of points of measure zero. At zero temperature, $\partial f(E_{\mathbf{k}}^{\alpha})/\partial E_{\mathbf{k}}^{\alpha}$ goes into a Dirac δ distribution, namely, $-\delta(E_{\mathbf{k}}^{\alpha})$. An equivalent term involving the superconducting state energies $E_s^{\alpha}(\mathbf{k})$ instead of the normal pseudogap energy $E_{\mathbf{k}}^{\alpha}$ would lead to zero contribution for the sum over the Brillouin zone momentum $\int d^2k/(2\pi)^2$. But, this is not the case for the normal state since the energies $E_{\mathbf{k}}^{\alpha}$ vanish on the Luttinger pockets [see Fig. 2(b)]. Our final formula for $H(x)$ is

$$H(x) = \frac{1}{\mathcal{N}}\int \frac{d^2k}{(2\pi)^2}\,\eta^4(\mathbf{k})\left\{\sum_{\alpha,\alpha'=\pm} W_{\mathbf{k}}^{\alpha}W_{\mathbf{k}}^{\alpha'}\left(\frac{E_{\mathbf{k}}^{\alpha}E_{\mathbf{k}}^{\alpha'}}{E_s^{\alpha}(\mathbf{k})E_s^{\alpha'}(\mathbf{k})} - 1\right)\frac{1}{E_s^{\alpha}(\mathbf{k}) + E_s^{\alpha'}(\mathbf{k})}\right.$$
$$\left. - 2\left[-\sum_{\alpha=\pm}\left(W_{\mathbf{k}}^{\alpha}\right)^2\delta\left(E_{\mathbf{k}}^{\alpha}\right) + 2W_{\mathbf{k}}^{+}W_{\mathbf{k}}^{-}\frac{\theta(E_{\mathbf{k}}^{-}) - \theta(E_{\mathbf{k}}^{+})}{E_{\mathbf{k}}^{+} - E_{\mathbf{k}}^{-}}\right]\right\}, \quad (17a)$$

with

$$\mathcal{N} = \int \frac{d^2k}{(2\pi)^2}\,\eta^4(\mathbf{k})\sum_{\alpha,\alpha'=\pm} W_{\mathbf{k}}^{\alpha}W_{\mathbf{k}}^{\alpha'}\frac{\Delta_{sc}^2(\mathbf{k},x)}{E_s^{\alpha}(\mathbf{k})E_s^{\alpha'}(\mathbf{k})\left[E_s^{\alpha}(\mathbf{k}) + E_s^{\alpha'}(\mathbf{k})\right]}, \quad (17b)$$

which is to be evaluated numerically as an integral over the CuO_2 Brillouin zone.

The numerical procedure to evaluate Eq. (17) involves the method of triangles, the two-dimensional (2D) version of the method of tetrahedrons,[53] using 21 504 triangles in the first BZ. Particular care is required for the three integrals involving Dirac's δ distribution because of the additional factor $\eta^4(\mathbf{k})$, which is strongly peaked around the X, Y, and commensurate points of the BZ [see Fig. 2(b)]. It is common practice in numerical work to replace the δ distribution by a Gaussian

$$\delta(x - x') = \lim_{\epsilon\to 0}\frac{1}{\epsilon\sqrt{\pi}}\exp\left[-\frac{(x-x')^2}{\epsilon^2}\right] \quad (18)$$

of width ϵ. If we only had to evaluate an integral of the type $\int d^2k/(2\pi)^2\,\delta(E_{\mathbf{k}}^{\alpha})$, we would then look for the number of triangles above which the value of the integral barely changes for a given width ϵ of the Gaussian and for the range $\epsilon \in [\epsilon_{\min},\epsilon_{\max}]$ within which the value of the integral remains stable under the variation of ϵ. An integral of the type $\int d^2k/(2\pi)^2\,\eta^4(\mathbf{k})\delta(E_{\mathbf{k}}^{\alpha})$, on the other hand, can not be expected to be stable against variation of ϵ because the left-hand tails of the Gaussian multiplied by $\eta^4(\mathbf{k})$ will now have more weight than their right-hand counterparts. In our numerical evaluation of Eq. (17), we treated the range $\epsilon \in [\epsilon_{\min},\epsilon_{\max}]$ for which the integral $\int d^2k/(2\pi)^2\,\delta(E_{\mathbf{k}}^{\alpha})$ remains stable against variation of ϵ to be "generic" to a certain $\delta(E_{\mathbf{k}}^{\alpha})$ and evaluated Eq. (17) separately for $\epsilon_{\min}$ and $\epsilon_{\max}$ treating the corresponding values of $H(x)$ as lower and upper boundaries to the "real" value of $H(x)$. This resulted in the error bars attached to the numerical data points [solid (black) squares] in Fig. 3. (In some cases, the error bars are of the size of the symbol.)

As the pseudogap opens for values of the hole doping just below the QCP at $x = x_c$, the Fermi surface reconstructs and both electron and hole Luttinger pockets appear. As x is decreased below approximately $x \simeq 0.17$ in our phase diagram, only hole pockets remain. As x is reduced further, the area of the remaining hole pockets shrinks. The superconducting gap also decreases in our model phase diagram [see Fig. 2(a)] in which we have taken it to be proportional to the critical-temperature dome. As the end of the dome closest to the antiferromagnetic Mott insulating state is approached,

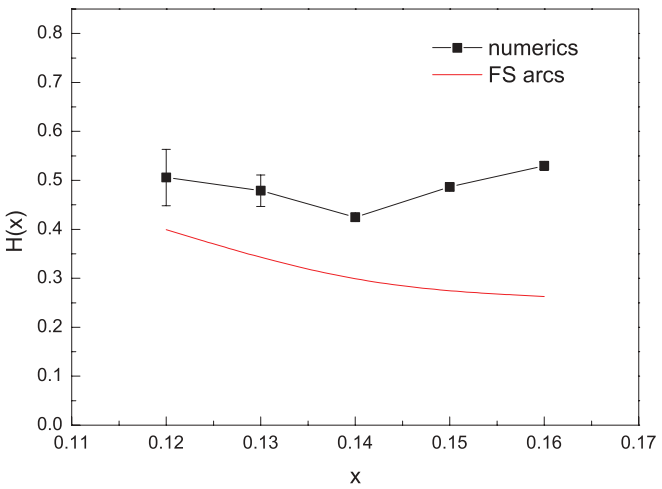

FIG. 3. (Color online) The doping dependence of $H(x)$ given in Eq. (4). $H(x) = 0$ gives an optical sum of $\frac{1}{2}$, while $H(x) = 1$ gives the conventional value of one. The solid squares are the result of complete calculations in the YRZ model, while the solid (red) curve gives the result based on the simplification to an arc model.

we expect that fluctuations will become important[54,55] and these are not part of the YRZ model. Therefore, in our numerics we limited ourselves to the range $0.12 \leqslant x \leqslant 0.16$. Our results are shown in Fig. 3 [solid (black) squares] where we see that $H(x)$ equals approximately 0.5 in this range giving $(N_s - N_n)/\rho_s \simeq 0.75$ rather than the value of one of Fermi-liquid theory. While the FGT sum rule is reduced in the YRZ model, it remains above the value of 0.5 found in experiment.[4]

Considerable insight into the variation of the FGT sum rule with nonzero pseudogap amplitude is obtained by studying in detail a simple limit of the YRZ model which results when the pseudogap is taken to open on the Fermi surface rather than away from it on a surface between Fermi surface and the antiferromagnetic BZ as it does in YRZ. This simplified "arc" model has the great virtue that we can obtain simple analytic results as we will see next, and this greatly helps in understanding the physics.

V. FERMI ARC MODEL

A great simplification of the YRZ model arises when we replace the antiferromagnetic BZ energy $\xi^0_{\mathbf{k}}$ in Eq. (7) by the band dispersion energy $\xi_{\mathbf{k}}$ in which case $E^{\pm}_{\mathbf{k}}$ reduces to $\pm E_{\mathbf{k}} \equiv \pm\sqrt{\xi^2_{\mathbf{k}} + \Delta^2_{pg}(\mathbf{k},x)}$ and $E^{\alpha}_s(\mathbf{k}) \equiv E_s(\mathbf{k}) = \sqrt{\xi^2_{\mathbf{k}} + \Delta^2_{sc}(\mathbf{k},x) + \Delta^2_{pg}(\mathbf{k},x)}$ independent of α. Applying these simplifications to Eq. (17) and accounting for the fact that in this case

$$\sum_{\alpha,\alpha'=\pm} W^{\alpha}_{\mathbf{k}} W^{\alpha'}_{\mathbf{k}} = 1 \tag{19}$$

and

$$(W^{+}_{\mathbf{k}})^2 + (W^{-}_{\mathbf{k}})^2 - 2W^{+}_{\mathbf{k}} W^{-}_{\mathbf{k}} = \frac{\xi^2_{\mathbf{k}}}{E^2(\mathbf{k})}, \tag{20}$$

we get for the first term in the numerator of Eq. (17) for $H(x)$

$$-\int \frac{d^2k}{(2\pi)^2}\, \eta^4(\mathbf{k}) \frac{\Delta^2_{sc}(\mathbf{k},x) + \Delta^2_{pg}(\mathbf{k},x)}{2E^3_s(\mathbf{k})}, \tag{21}$$

and for the denominator

$$\int \frac{d^2k}{(2\pi)^2}\, \eta^4(\mathbf{k}) \frac{\Delta^2_{sc}(\mathbf{k},x)}{2E^3_s(\mathbf{k})}. \tag{22}$$

The second term in the numerator of Eq. (17) works out to be

$$\int \frac{d^2k}{(2\pi)^2}\, \eta^4(\mathbf{k}) \Bigg[\sum_{\alpha=\pm} \left(W^{\alpha}_{\mathbf{k}}\right)^2 \left(-2\frac{\partial f(E_{\mathbf{k}})}{\partial E_{\mathbf{k}}} \right) + 4W^{+}_{\mathbf{k}} W^{-}_{\mathbf{k}} \frac{1 - 2f(E_{\mathbf{k}})}{2E_{\mathbf{k}}} \Bigg]. \tag{23}$$

Next, we take the continuum limit for the energy bands in which the approximation $\int d^2k/(2\pi)^2 = N(0)\int_{-\infty}^{\infty} d\xi \int_0^{(2\pi)} d\theta/(2\pi)$ and the integral over energy ξ can be done. Here, $N(0)$ is the electronic band density of states assumed constant throughout the infinite band. As part of this same model, the tunneling factor $\eta(\mathbf{k}) = \cos(2\theta)$ and $\Delta_{sc}(\mathbf{k},x)$ and $\Delta_{pg}(\mathbf{k},x)$ become $\Delta^0_{sc}(x)\cos(2\theta)$ and $\Delta^0_{pg}(x)\cos(2\theta)$, respectively. This simplified band model is illustrated in Fig. 4. It shows a circular Fermi surface with Fermi arc (on which

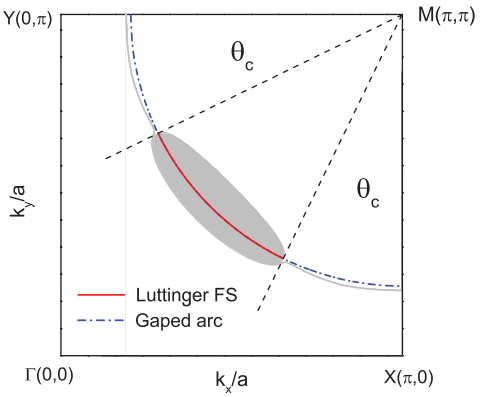

FIG. 4. (Color online) Arc model for Luttinger pockets [shaded (gray) region]. The two sides of the shaded region are Fermi surfaces and the gray line beyond is a contour of closest approach which is gaped. The Fermi contour in the arc model is the solid (red) line with $\theta \in [\pi/4,\theta_c]$ and the dashed-dotted (blue) is the extension but with a gap.

there are zero-energy excitations) restricted to the region $\theta \in [\theta_c,\pi/2 - \theta_c]$ and the remainder of their circle is gaped in the regions $\theta \in [0,\theta_c)$ and $\theta \in (\pi/2 - \theta,\pi/2]$. We will use the fact that $\int_{-\infty}^{\infty} d\xi\, \Delta^2/(\Delta^2 + \xi^2)^{(3/2)} = 2$ for any value of Δ. Applying this rule to Eqs. (21) and (22) gives explicitly

$$-\int_0^{\pi/4} d\theta\, \cos^4(2\theta) \tag{24}$$

and

$$\int_{\theta_c}^{\pi/4} d\theta \cos^4(2\theta) + \frac{\left[\Delta^0_{sc}(x)\right]^2}{\left[\Delta^0_{sc}(x)\right]^2 + \left[\Delta^0_{pg}(x)\right]^2} \int_0^{\theta_c} d\theta \cos^4(2\theta), \tag{25}$$

where we left out common factors which will drop out of the ratios in Eq. (17) for $H(x)$. The term (23) needs to be treated with special care as its value depends critically on the value of θ, i.e., whether it is within the interval $[\theta_c,\pi/2 - \theta_c]$ about the nodal direction where the Fermi surface exists, or on the remaining part of the Fermi circle where the contour is gaped out by the pseudogap. We get

$$\int_0^{\theta_c} d\theta\, \cos^4(2\theta) + 2\int_{\theta_c}^{\pi/4} d\theta\, \cos(2\theta), \tag{26}$$

with the first term coming from the second term in Eq. (23) and the second term from the Dirac δ distribution $-\partial f(E)/\partial E = \delta(E)$ as $T \to 0$. This leads to our final approximate result

$$H(\theta_c) = \frac{\int_{\theta_c}^{\pi/4} d\theta\, \cos^4(2\theta)}{\int_{\theta_c}^{\pi/4} d\theta\, \cos^4(2\theta) + \frac{1}{1+[\Delta^0_{pg}(x)/\Delta^0_{sc}(x)]^2} \int_0^{\theta_c} d\theta\, \cos^4(2\theta)}. \tag{27}$$

For no pseudogap, $\theta_c \to 0$ and we get one for $H(\theta_c)$ in Eq. (27) and so recover the conventional sum rule of one. For a large pseudogap, $\theta_c \to \pi/4$ (very small Luttinger pockets) the numerator of Eq. (27) goes to zero and the denominator remains finite in the range where $\Delta^0_{sc}(x)$ is finite and so we get $H(x) = 0$ and the sum rule is now equal to 0.5. In general, θ_c remains finite within the superconducting dome and, thus,

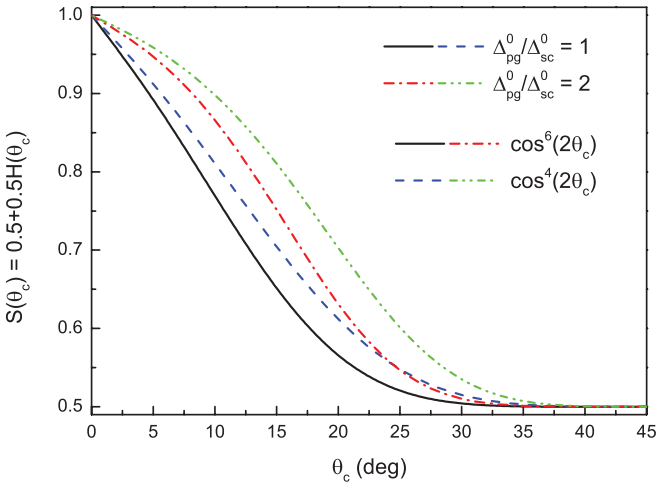

FIG. 5. (Color online) The sum rule of Eq. (4) with $S(\theta_c) \equiv (N_n - N_s)/\rho_s$ as a function of the arc cutoff θ_c (see Fig. 4) for two assumptions in the treatment of the transverse tunneling matrix element. The dashed (blue) and dashed-double dotted (green) lines are for a cosine to the fourth power as in Eq. (3) in the continuum limit and the solid (black) and dashed-dotted (red) lines, which are presented only for comparison, are for a cosine to the sixth power. The solid (black) and dashed (blue) curves are for $\Delta^0_{pg}/\Delta^0_{sc} = 1$, while the dashed-dotted (red) and dashed-double dotted (green) lines are for a case when this ratio is equal to two.

the sum rule will be larger than 0.5 but less than one in line with our full numerical calculations. The arc model, however, allows us to make estimates of the magnitude of the optical sum rule not tied directly to the parameters that were used in the original paper by Yang *et al.*[21] A reasonable set of parameters could be an arc of $\theta_c = 30^\circ$ and a pseudogap twice the value of the superconducting gap. In this case, $H(\theta_c) = 0.055$ and the optical sum of the system becomes according to Eq. (26) approximately 0.53, very nearly 0.5. It is clear that with reasonable parameters, not constrained to the set used by YRZ, one can obtain a sum rule near the observed value reported by Basov *et al.*[4] On the other hand, if we take parameters for the arc model through a fit to the work of YRZ as we did in the solid (red) curve in our Fig. 3, we get a higher value of the sum rule. This implies that changes in the parameter set used in Ref. 21 are required to get agreement with present experiments. In making such comparisons, experimental error, which increases as the conductivity decreases in magnitude, should also be kept in mind. We make a final point. The form of the tunneling matrix element (3) also influences the quantitative values of the c-axis optical sum as can be seen in Fig. 5. In this plot, we give results for the sum rule $S(\theta_c) \equiv (N_n - N_s)/\rho_s$ of Eq. (4) as a function of the angular cutoff θ_c of the arc model (see Fig. 4). No constraint has been imposed on the size of θ_c for a given value of the pseudogap amplitude Δ^0_{pg}. The solid (black) and dashed-dotted (red) curves apply to the case when the tunneling matrix element squared has a $\cos^6(2\theta)$ dependence rather than the fourth power [dashed (blue) and dashed-double dotted (green) curves]. Two values of the pseudogap to superconducting gap amplitude $\Delta^0_{pg}/\Delta^0_{sc}$ are shown with the solid (black) and dashed-dotted (red) curves for $\Delta^0_{pg}/\Delta^0_{sc} = 1$ and the dashed (blue) and dashed-double dotted (green) curves for a ratio of two. It is clear that the numerical value for $S(\theta_c)$ does depend on the form of the transverse transfer matrix element and is smaller for the higher power of the cosine. The qualitative dependence of the sum rule, however, is not strongly modified.

VI. SUMMARY AND CONCLUSION

In underdoped cuprates, in the pseudogap state, the transverse c-axis optical conductivity perpendicular to the CuO_2 planes does not obey the usual FGT sum rule. Rather, the ratio of the missing area under the real part of the optical conductivity between normal and superconducting phases is observed to be closer to half of the c-axis superfluid density than to the more conventional value of one. Here, we present a numerical evaluation of this sum rule within the recent pseudogap model of YRZ who provide an ansatz for the system Green's function as well as for its Gor'kov anomalous counterpart, which is phenomenological, although grounded in the ideas of the resonating valence bond spin liquid. Without making any adjustments to the set of parameters set out in Ref. 21 as an illustration, and based on considerations of the bands in $Ca_2CuO_2Cl_2$, our numerical evaluation gives a sum rule of order 0.75, which falls between the measured value of 0.5 and the conventional value of one for the FGT sum rule. The model also predicts a variation of the sum rule with doping.

We show that simple analytic formulas can be obtained in a limit of the YRZ model, which reduces to the well-known Fermi arc model. In this model, there is a Fermi surface centered on the antinodal direction but its extent is limited to an arc beyond which there is a gap on the remaining contour of Fermi-liquid theory. The formula so obtained is very simple and allows one to make estimates of the FGT sum rule for parameters characterizing the pseudogap which are not tied to those in the original formulation of YRZ. The formula involves only the tunneling matrix element between planes, the ratio between superconducting and pseudogap amplitude, and the angular length of the Fermi surface arc. It is clear that a sum rule between $\geqslant 0.5$ and one is easily obtained for a range of reasonable values for the parameters involved and that a FGT sum greater than one half but significantly less than one is generic to the YRZ model.

ACKNOWLEDGMENT

Research was supported in part by the Natural Sciences and Engineering Research Council of Canada (NSERC) and by the Canadian Institute for Advanced Research (CIFAR).

*schachinger@itp.tu-graz.ac.at

[1] E. Schachinger and J. P. Carbotte, J. Low Temp. Phys. **144**, 61 (2006).
[2] R. A. Ferrell and R. E. Glover, Phys. Rev. **109**, 1398 (1958).
[3] M. Tinkham and R. A. Ferrell, Phys. Rev. Lett. **2**, 331 (1959).

[4]D. N. Basov, S. I. Woods, A. S. Katz, E. J. Singley, R. C. Dynes, M. Xu, D. G. Hinks, C. C. Homes, and M. Strongin, Science **283**, 49 (1999).
[5]W. Kim and J. P. Carbotte, Phys. Rev. B **61**, R11886 (2000).
[6]W. Kim and J. P. Carbotte, Phys. Rev. B **62**, 8661 (2000).
[7]J. Hirsch, Physica C (Amsterdam) **199**, 305 (1992).
[8]L. Ioffe and A. Millis, Science **285**, 1241 (1999).
[9]J. Hirsch, Physica C (Amsterdam) **201**, 347 (1992).
[10]P. W. Anderson, Science **279**, 1196 (1998).
[11]S. Chakravarty, Eur. Phys. J. B **5**, 337 (1998).
[12]S. Chakravarty, H.-Y. Kee, and E. Abrahams, Phys. Rev. Lett. **82**, 2366 (1999).
[13]W. Kim and J. P. Carbotte, Phys. Rev. B **63**, 054526 (2001).
[14]W. Kim and J. P. Carbotte, Phys. Rev. B **64**, 104501 (2001).
[15]T. Timusk and B. Statt, Rep. Prog. Phys. **62**, 61 (1999).
[16]S. Hüfner, M. Hossain, A. Damascelli, and G. A. Sawatzky, Rep. Prog. Phys. **71**, 062501 (2008).
[17]V. Emery and S. Kivelson, Nature (Lonodon) **374**, 434 (1995).
[18]M. Randeria, N. Trivedi, A. Moreo, and R. T. Scalettar, Phys. Rev. Lett. **69**, 2001 (1992).
[19]S. Chakravarty, R. B. Laughlin, D. K. Morr, and C. Nayak, Phys. Rev. B **63**, 094503 (2001).
[20]J.-X. Zhu, W. Kim, C. S. Ting, and J. P. Carbotte, Phys. Rev. Lett. **87**, 197001 (2001).
[21]K.-Y. Yang, T. M. Rice, and F.-C. Zhang, Phys. Rev. B **73**, 174501 (2006).
[22]B. Valenzuela and E. Bascones, Phys. Rev. Lett. **98**, 227002 (2007).
[23]E. Illes, E. J. Nicol, and J. P. Carbotte, Phys. Rev. B **79**, 100505(R) (2009).
[24]J. P. Carbotte, K. A. G. Fisher, J. P. F. LeBlanc, and E. J. Nicol, Phys. Rev. B **81**, 014522 (2010).
[25]J. P. F. LeBlanc, E. J. Nicol, and J. P. Carbotte, Phys. Rev. B **80**, 060505 (2009).
[26]K.-Y. Yang, H.-B. Yang, P. Johnson, T. Rice, and F.-C. Zhang, Europhys. Lett. **86**, 37002 (2009).
[27]J. P. F. LeBlanc, J. P. Carbotte, and E. J. Nicol, Phys. Rev. B **81**, 064504 (2010).
[28]A. J. H. Borne, J. P. Carbotte, and E. J. Nicol, Phys. Rev. B **82**, 024521 (2010).
[29]K.-Y. Yang, K. Huang, W.-Q. Chen, T. M. Rice, and F.-C. Zhang, Phys. Rev. Lett. **105**, 167004 (2010).
[30]H.-B. Yang, J. D. Rameau, Z.-H. Pan, G. D. Gu, P. D. Johnson, H. Claus, D. G. Hinks, and T. E. Kidd, Phys. Rev. Lett. **107**, 047003 (2011).
[31]A. Pound, J. P. Carbotte, and E. J. Nicol, Eur. Phys. J. B **81**, 69 (2011).
[32]P. W. Anderson, Science **235**, 1196 (1987).
[33]J. P. Carbotte, F. Marsiglio, and B. Mitrović, Phys. Rev. B **33**, 6135 (1986).
[34]F. Marsiglio, R. Akis, and J. P. Carbotte, Phys. Rev. B **45**, 9865 (1992).
[35]B. Mitrović, C. R. Leavens, and J. P. Carbotte, Phys. Rev. B **21**, 5048 (1980).
[36]D. Branch and J. P. Carbotte, Phys. Rev. B **52**, 603 (1995).
[37]C. O'Donovan and J. P. Carbotte, Phys. Rev. B **52**, 16208 (1995).
[38]H. K. Leung, J. P. Carbotte, D. W. Taylor, and C. R. Leavens, Can. J. Phys. **54**, 1585 (1976).
[39]E. Schachinger, M. G. Greeson, and J. P. Carbotte, Phys. Rev. B **42**, 406 (1990).
[40]P. Arberg, M. Mansor, and J. P. Carbotte, Solid State Commun. **86**, 671 (1993).
[41]B. Mitrović and J. P. Carbotte, Can. J. Phys. **61**, 758 (1983).
[42]B. Mitrović and J. P. Carbotte, Can. J. Phys. **61**, 784 (1983).
[43]R. J. Radtke, V. N. Kostur, and K. Levin, Phys. Rev. B **53**, R522 (1996).
[44]E. H. Kim, Phys. Rev. B **58**, 2452 (1998).
[45]R. J. Radtke and K. Levin, Physica C (Amsterdam) **250**, 282 (1995).
[46]P. J. Hirschfeld, S. M. Quinlan, and D. J. Scalapino, Phys. Rev. B **55**, 12742 (1997).
[47]M. V. Klein and G. Blumberg, Science **283**, 42 (1999).
[48]S. Chakravarty, A. Subo, P. W. Anderson, and S. Strong, Science **261**, 337 (1993).
[49]O. K. Anderson, A. I. Liechtenstein, O. Jepen, and F. Paulsen, J. Phys. Chem. Solids **56**, 1573 (1995).
[50]T. Xiang and J. M. Wheatley, Phys. Rev. Lett. **77**, 4632 (1996).
[51]T. Xiang, C. Panagopoulos, and J. R. Cooper, Int. J. Mod. Phys. B **12**, 1007 (1998).
[52]K. G. Sandeman and A. J. Schofield, Phys. Rev. B **63**, 094510 (2001).
[53]G. Lehmann and M. Taut, Phys. Status Solidi B **54**, 469 (1972).
[54]M. Franz and A. J. Millis, Phys. Rev. B **58**, 14572 (1998).
[55]T. Eckl, D. J. Scalapino, E. Arrigoni, and W. Hanke, Phys. Rev. B **66**, 140510 (2002).